Coupled modelling and sampling approaches to assess the impacts of human water management on land-sea carbon transfer

Shaoqiang Ni [a], Xiao Huang [b,*], Weixiu Gan [a], Conrad Zorn [c], Yuchen Xiao [a], Guorui Huang [a]
Chaoqing Yu [a,d,*], Jifu Cao [e], Jie Zhang [f], Zhao Feng [a], Le Yu [a], Guanghui Lin [a], Hanna Silvennoinen [g]

[a] Department of Earth System Science, Ministry of Education Key Laboratory for Earth System Modeling, Tsinghua University, Beijing 100084, China
[b] Norwegian Institute of Bioeconomy Research, Saerheim, 4353, Norway
[c] Environmental Change Institute, University of Oxford, Oxford OX1 3QY, UK
[d] AI for Earth Laboratory, Cross-strait Tsinghua Research Institute, Xiamen 361000, China
[e] Zhanjiang Hydrology Branch of Guangzhou Hydrology Bureau, Zhanjiang 524000, China
[f] Key Laboratory for Geo-Environmental Monitoring of Coastal Zone (GEMCO) of the National Administration of Surveying, Mapping and GeoInformation, Shenzhen University, Shenzhen 518060, China
[g] Norwegian Institute of Bioeconomy Research, Ås 1430, Norway

HIGHLIGHTS

- An integrated framework for the quantification of land-sea carbon transfer is presented.
- The riverine carbon in the study area is dominated by water volume of runoff rather than carbon concentration.
- Human impacts can reduce a significant proportion of the land-sea riverine carbon transfer at both annual and seasonal scale.
- Natural factors like seasonal drought can markedly enhance human impact by stricter water management strategies.

GRAPHICAL ABSTRACT
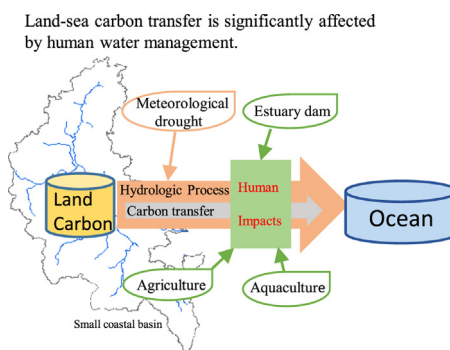
Land-sea carbon transfer is significantly affected by human water management.

ARTICLE INFO

ABSTRACT

Land-sea riverine carbon transfer (LSRCT) is one of the key processes in the global carbon cycle. Although natural factors (e.g. climate, soil) influence LSRCT, human water management strategies have also been identified as a critical component. However, few systematic approaches quantifying the contribution of coupled natural and anthropogenic factors on LSRCT have been published. This study presents an integrated framework coupling hydrological modeling, field sampling and stable isotope analysis for the quantitative assessment of the impact of human water management practices (e.g. irrigation, dam construction) on LSRCT under different hydrological conditions. By applying this approach to the case study of the Nandu River, China, we find that carbon (C) concentrations originating from different land-uses (e.g. forest, cropland) are relatively stable and outlet C variations are mainly dominated by controlled runoff volumes rather than by input C concentrations. These results indicate that human water management practices are responsible for a reduction of ~60% of riverine C at seasonal timescales, with an even greater reduction during drought conditions. Annual C discharges have been significantly reduced (e.g. 77 ± 5% in 2015 and 39 ± 11% in 2016) due to changes in human water extraction coupled with climate variation. In addition, isotope analysis also shows that C fluxes influenced by human activities

* Corresponding authors at: Norwegian Institute of Bioeconomy Research, Saerheim, 4353, Norway (X. Huang). Department of Earth System Science, Ministry of Education Key Laboratory for Earth System Modeling, Tsinghua University, Beijing 100084, China (C. Yu).
E-mail addresses: xiao.huang@nibio.no (X. Huang), chaoqingyu@yahoo.com (C. Yu).

(e.g. agriculture, aquaculture) could contribute the dominant particulate organic carbon under typical climatic conditions, as well as drought conditions. This research demonstrates the substantial effect that human water management practices have on the seasonal and annual fluxes of LSRCT, especially in such small basins. This work also shows the applicability of this integrated approach, using multiple tools to quantify the contribution of coupled anthropogenic and natural factors on LSRCT, and the general framework is believed to be feasible with limited modifications for larger basins in future research.

1. Introduction

The transportation of sediment and nutrients from land to ocean is one of the crucial processes in the earth system dynamics (Walling, 2006; Alin et al., 2011; Bouwman et al., 2013). Land-sea riverine carbon transfer (LSRCT), as an important component of the global carbon (C) cycle, may not only supply C resources to the food web of coastal and offshore aquatic ecosystems (Darnaude, 2005), but also trigger environmental problems such as eutrophication and hypoxia (Lenton, 2000; Chen and Swaney, 2012). Globally, riverine C transfers to the sea as DIC (Dissolved Inorganic Carbon), DOC (Dissolved Organic Carbon) and POC (Particular Organic Carbon) are estimated to be on the order of 0.25–0.36 PgC yr^{-1}, 0.20 PgC yr^{-1} and 0.41 PgC yr^{-1}, respectively (Meybeck, 1982; Aitkenhead and Mcdowell, 2000; Cai et al., 2015). This is a significant contribution towards the terrestrial carbon sink, which is estimated at 2.0–3.4 PgC yr^{-1} (Canadell et al., 2007; Quéré et al., 2009; Pan et al., 2011). A comprehensive understanding of the LSRCT process could improve our ability to manage aquatic ecosystems and estimate the global C cycle under the influence of human activities and climate change.

Previous studies have assessed the LSRCT in different carbon forms (e.g. DIC, DOC, POC) under the influence of natural factors, such as hydrological and meteorological conditions (Raymond et al., 2008; Hruška et al., 2009). For example, studies over major American rivers have shown that LSRCT is mainly controlled by runoff processes rather than carbon sources supply, due to the consistent change between carbon fluxes and water runoff (Raymond and Oh, 2007; Raymond et al., 2008). In addition, a study in the Pearl River Delta found a correlation between the total organic carbon transfer and rainfall/river discharges (Ni et al., 2008). However, most of these studies have concentrated on estimating the order of magnitude of the LSRCT, in some of the world's larger river basins as well as in smaller-scale river basins. These larger basins included for example the Amazon River (Richey et al., 1990), the Mississippi River (Green et al., 2006), the Pearl River (Ni et al., 2008), the Yangtze River (Wu et al., 2007) and the Lena and Yenisey Rivers (Dittmar and Kattner, 2003; Semiletov et al., 2011). Smaller basins include the Bohai Sea (Xia and Zhang, 2011), Dominica (Mondro, 2010), southwest Tahiti (Mcgillis et al., 2015) and Panama (Goldsmith et al., 2015). While the importance of quantifying LSRCT is recognized globally, few studies consider how humans affect the complicated transfer process. In recent studies however, human impact has become the subject of greater focus (Regnier et al., 2013).

With economic development and population growth, the increasing demands on fresh water resources for agricultural, domestic and industrial use, as well as energy production, have motivated significant alterations of natural river systems in many places, through damming, channel realignment and bulk water abstractions (Loucks and Van Beek, 2017). For example, we manually identified the rivers of China using high-resolution satellite imagery, and the results showed that 86% of 138 identifiable rivers from the southwest of Guangxi Province to the northeast of Liaoning Province feature estuary dams (see Fig. S1). Globally the impact

of human perturbation on LSRCT has been estimated as an increase of 0.1 PgC yr^{-1} to open oceans since pre-industrial times (Regnier et al., 2013), with increased urbanization responsible for 90% of the long-term rise in fluvial DOC (Noacco et al., 2017). At more localized scales, the impact of human activities on transport processes and seasonal variations of organic carbon transport have been estimated using field investigation data in the Yellow River in China (Zhang et al., 2013) and multi-year model simulations have been applied in eastern North America to estimate the anthropogenic and climatic influences on LSRCT (Tian et al., 2015). Nevertheless, such applications either focus on a particular aspect of human perturbation (e.g. fertilization) without a holistic assessment, or simply provide a qualitative analysis of the varying trends of riverine carbon.

Although the single approach of either hydrological modeling, field sampling and isotope analysis has been used in a wide range of areas, including the LSRCT, each approach has its own limitations and shortcomings. Firstly, C field sampling is frequently used to provide accurate C concentration values, followed by the determination of C fluxes under different environmental factors (Wu et al., 2007; Ran et al., 2013; Marques et al., 2017). However, this method has a relatively low spatial-temporal frequency due to the heavy workload involved in manual sampling and the complicated post-treatment processes. In addition, field sampling is not capable of predicting the C concentration variation under possible future scenarios, such as climate and land-use changes. Besides the magnitude of C fluxes, further C management at the basin scale also requires a determination of the contributions from different sources (e.g. forest and cropland), based on which optimal practices could be performed effectively. Stable isotope analysis is a widely used tool in studying the water flow and pollution sources for land water and seawater intrusion (Wassenaar et al., 2011; Mahlknecht et al., 2017). This method has recently been applied largely in tracing the riverine C sources for the river food web (Pingram et al., 2012; Csank et al., 2019). However, this method cannot be used to determine the exact quantity of transferred C, nor to predict the change tendency of C sources for future C management. Generally, stable isotope analyses must be combined with other methods. On the other hand, hydrological model simulations have the ability to quantify the flow dynamics and solution migration. For example, the SWAT model has been used in local watersheds to estimate the surface runoff and soil erosion, and thus the sediment simulation (Tibebe and Bewket, 2011). The prediction of runoff and sediment yield in a small agricultural basin has also been evaluated with the AnnAGNPS model (Chahor et al., 2014). However, although these models typically show good accuracy in water flow simulations, they are weaker with respect to the sediment and carbon assessment due to the poorly understood mechanisms and large spatial heterogeneity. It is precisely due to the overdependence on vast empirical equations and parameters that these modeling methods remain highly uncertain (Tian et al., 2015; Li et al., 2017).

As the impacts of human activities coupled with natural factors on the LSRCT remain incompletely understood and the aforementioned single methods have individual shortcomings, an integrated

framework incorporating the advantages of all of these methods is therefore required. For example, each method may play a different role within the integrated framework, with hydrological modeling allowing the accurate simulation of water runoff processes, field sampling providing C concentration values at key points for C flux calculations, and stable isotope analysis tracing the contribution of different C sources. In addition, the integrated framework is expected to have the following features: (a) the ability to replicate historical C transfer processes to assess the human impact on LSRCT and make predictions for future C transfer change tendencies with longer time sequences and a higher resolution, (b) the ability to provide effective support for human water and C management for the purposes of policy setting and environmental protection, and (c) an improved assessment accuracy compared to single-method approaches.

As a result of these considerations, this paper sets out an integrated quantitative approach incorporating hydrological modeling, field sampling and stable isotope analysis to assess human impacts on LSRCT. To verify the effectiveness of this integrated approach, we conduct a case study in the Nandu River Basin (China). The application of this framework to the case study allows us to answer the following questions: (i) To what extent could human water management strategies impact the riverine C input sources; (ii) How do coupled drought conditions and human water management practices impact the LSRCT flux; and (iii) What is the ratio of carbon sources that are under human water management practices controlling.

We begin by outlining our approach in Section 2, including the methodology and experimental workflow used to evaluate the LSRCT. In Section 3, we introduce our application of the approach in the Nandu River basin in Leizhou Peninsula, China, which constitutes a representative coastal basin in East and Southeast Asia. We then describe the detailed implementation of the approach: (A) the development and calibration/validation of the basin hydrological model, (B) the laboratory testing of water and vegetation samples taken over multiple years across the river basin, and (C) the coupling of datasets to quantify carbon fluxes under both normal and severe drought conditions. In Section 4, we present the results and a drought frequency analysis to evaluate the overall impact of water management practices. Finally, in Sections 5 and 6 we present the conclusions of our analysis with respect to the research questions posed and discuss the limitations of our study, as well as possible modifications to the general framework for applications in future research in different coastal basins.

2. Methodology

2.1. Basic mechanism of LSRCT

A simplified Water-C system diagram is presented in Fig. 1, and is representative of what could be observed along coastal basins such as the Nandu River basin in China (see Section 3).

In such coastal basins, the runoff or discharges from agriculture (i.e. cropland), aquaculture (i.e. fishponds at fish farms), domestic use areas (water consumption), forests, the atmosphere and other basins all contribute carbon to the river network and finally, via an outlet (i.e. sluice gate), to the ocean. Inland feedback loops exist, for example where river water (and associated nutrients and carbon) are pumped back to croplands for irrigation purposes, which in turn return to the water system via overland flow and/or groundwater. Similar water/C transfers occur between fishponds at fish farms and in domestic use. Extractions of water (and therefore C) and discharges back to the river system after agricultural, aquacultural and domestic uses are all typically human-controlled, with the exception of natural runoff. The atmosphere contributes to the C cycle through gas (CO_2) exchange processes, mainly influenced by the flow conditions and air pressure. At the downstream end of Fig. 1, the damming of water and controlled release affects the natural flow process through changes to evaporation and discharge rates. Generally, these relationships are poorly understood given the complexity of the carbon cycle and feedback loops, and therefore require more in-depth research and closer coupling of water quality measurements and hydrologic water resources models. The following section outlines our methodology for the study of the coupled system.

2.2. Approach and experimental design

Fig. 2 presents our approach and experimental design for evaluating LSRCT in a coastal river basin catchment. There are three main components: (A) the hydrological modeling of the system, (B) the collection of water and vegetation samples for laboratory analysis to identify the sources and concentrations of riverine C, and (C) the integration of the validated hydrologic model of the catchment with field sampling results to assess and quantify the impacts that human water management strategies have on the natural riverine C cycle.

The first stage of the analysis, labeled (i) in Fig. 2, involves generating a computationally efficient and accurate representation of the hydrology of the wider river catchment. For this analysis, we adopt the 'Soil and Water Assessment Tool' (SWAT model) developed by the United States Department of Agriculture-Agricultural Research Service (USDA-ARS). This is a distributed-parameter, process-based hydrological model common across the literature for basin-scale runoff and water quality modeling (Srinivasan et al., 1998; Santhi et al., 2010). Critical to the SWAT model is the division of a catchment into smaller hydrological response units (HRU) representing spatially continuous sub-catchments with an assumed homogeneous hydrological response, for example similar soil types and land uses. In addition to such underlying soil and land use data, ground topography and observed precipitation, river flow and flow control data are required over extended time periods for sufficient calibration and validation of the model. Many applications (Gikas et al., 2006; Setegn et al., 2010; Lin et al., 2015; Dutta and Sen, 2018) have been published using this model, with ongoing improvements enhancing model reliability (Zhang et al., 2005; Zhang et al., 2015).

Secondly (Component ii, Fig. 2), physical water sampling with adequate temporal (i.e. grasping the significant turning points) and spatial (i.e. distributed over a typical river section) representation is required to determine the isotope signals and concentration values of POC, DOC, and DIC at the sampling sites. Vegetation sampling is also performed to enable stable isotope analysis for the identification of C sources from the range of different land uses/vegetation types in the catchment.

Finally (Component iii, Fig. 2), the hydrological catchment modeling and data regarding the outlet control operations are integrated with the experimentally measured C concentrations to allow the quantification of LSRCT, both for conditions with (i.e. current conditions) and without (i.e. natural conditions) control structures and human modifications across the catchment.

3. Application to the Nandu river basin

3.1. Catchment overview

The Nandu River Basin (Fig. 3) is the largest river basin within the Leizhou Peninsula (Guangdong Province, China), with a catchment area of ~1444 km^2 and an annual average water resource of ~866 million m^3 (Peng et al., 2002). The main stream has a length
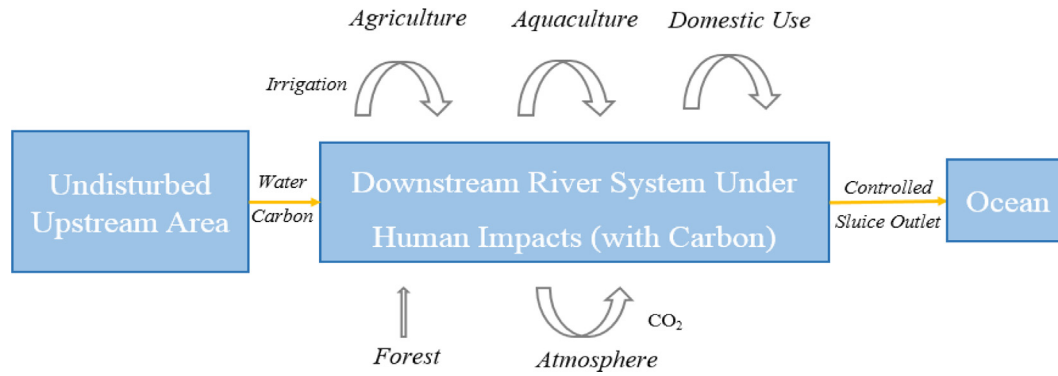
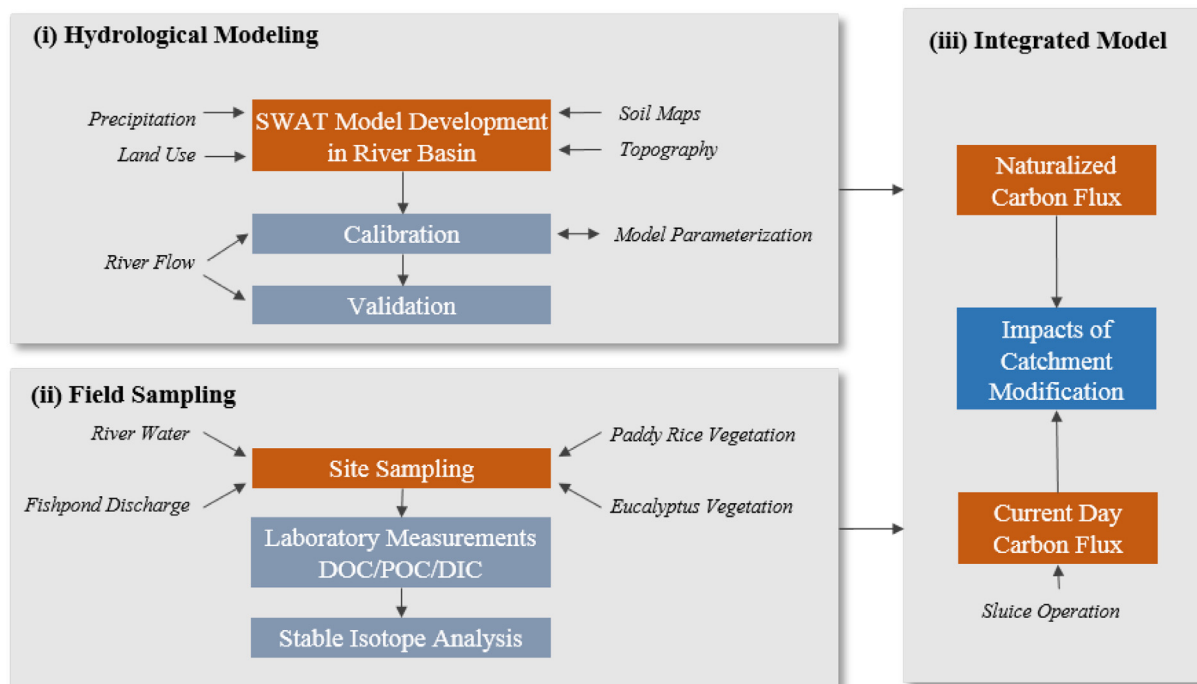**Fig. 1.** Simplified diagram of water and C transfer in a coastal basin.

Fig. 2. Workflow design of the proposed approach for integrating hydrologic modeling with field sampling and laboratory measurements.

of 88 km and the change in elevation across the catchment is 226 m (Fig. S2a). The dominant land uses in the river basin are rice paddies and eucalyptus forests, accounting for over 75% of the land area (Fig. S2c). Alluvial clays, including paddy soil and latosolic red soil, form the majority of the underlying soils (Fig. S2d). The coastal area features a number of ponds used for aquaculture (fish farming) and mangroves in tidal zones. The hydrology of the rice paddies and fishponds is strictly controlled via management by their respective owner/operators.

A single hydro-meteorological station (Duling Station, Fig. 3) is located in the Gongheshui tributary of the greater Nandu River basin. The next closest station is located near the city of Zhanjiang, approximately 35 km east of the upper reaches of the Nandu basin. The average annual precipitation across the catchment is ~1640 mm and is among the highest in mainland China. However, unstable monsoon rain and subtropical high pressure systems result in frequent seasonal droughts.

The Nandu River Dam, constructed in 1972 (Qin and Chen, 2011), is located at the sluice outlet of the main river system in the river basin (marked as Sluice Outlet in Fig. 3) and is an important flow control structure for managing water resources in the basin. Water can be pumped from the dam reservoir for irrigation in the wider catchment or released via the controlled operation of the sluice gate. The LSRCT is highly controlled by the operation of the sluice gate. The water level in the reservoir is kept lower in the rainy season to facilitate the discharge of floodwater, but higher in the dry season to store more freshwater resources. During droughts, the sluice gate is strictly controlled to reduce water discharge, which is conducive to the accumulation of the C concentration in the reservoir. A greater amount of riverine C will therefore be pumped back to the croplands during droughts because of the higher agricultural water consumption from the reservoir, which has a comparatively higher C concentration. When a drought ends, the remaining water in the reservoir is mixed with newly incoming water and discharged into the sea. During the rainy season, the C concentration is maintained at a relatively stable low value due to the more frequent flushing of the reservoir.
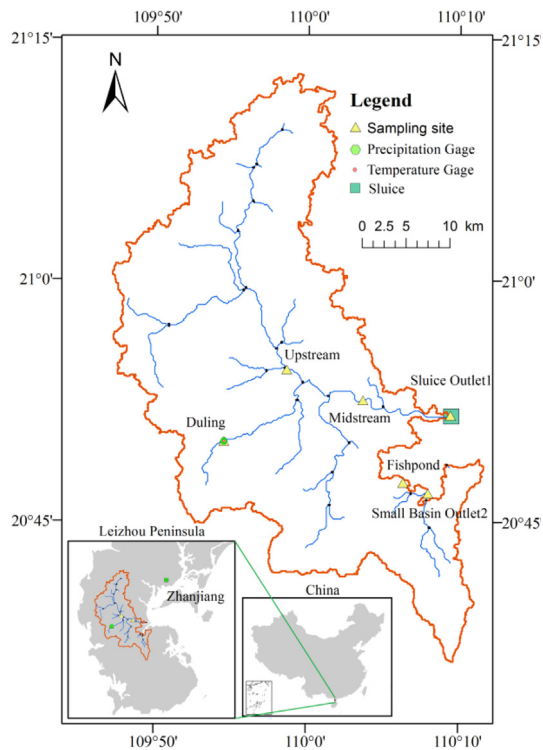
Fig. 3. Overview of the Nandu River Basin, showing climate measurement sites, water sampling sites and points of interest. The inset maps show the catchment location with respect to Zhanjiang City on the Leizhou Peninsula, and within Greater China.

3.2. Hydrological model development

3.2.1. Input data and post-processing

A range of data sources have been used to develop the SWAT model of the Nandu River basin. An overview of the datasets and their sources is provided in Table 1.

Of these datasets, the topography, land use and soil maps (as presented in Fig. S2) were obtained from open sources and used to delineate the HRUs. Input climate data was taken from two climate stations (Fig. 3). Duling station climate data were collated for short term records (2014–2016) with the purpose of model calibration/validation. At the nearby Zhanjiang station, 62 years of historic precipitation records from 1955 to 2016 were used to compute the widely accepted index return period to evaluate the severity of droughts (Lanen et al., 2016; Volpi et al., 2016).

Observed river flows were adopted from the Duling station for the purpose of model calibration/validation. The operation data of the sluice outlet (location shown in Fig. 3) and the daily water level observations were used to estimate the total catchment run-off volume, V_{inflow} (the inflow to the reservoir behind the sluice), through a daily water balance, such that:

$$V_{inflow} = \left(V_{outflow} + V_{leakage} + V_{extract}\right) - P + E + \Delta V_{reservoir} \tag{1}$$

where $V_{outflow}$ is the observed discharge from the sluice to the ocean provided by the sluice management data, $V_{leakage}$ is the reservoir leakage that can be neglected in small catchments where the water head is relatively small, $V_{extract}$ is the volume extracted for other purposes (irrigation, domestic use), P is the precipitation volume added to the reservoir, E is the evaporation water volume, and $\Delta V_{reservoir}$ is the change in reservoir volume, with the reservoir volume $V_{reservoir}$ defined by the reservoir stage-volume relationship:

$$V_{reservoir} = -24.74h^4 + 279.37h^3 - 669.03h^2 + 1750.50h$$
$$+ 4095.30 \tag{2}$$

where h is the observed water level. The derivation of this relationship is provided in Fig. S4.

Based on the general practices of the Nandu River basin, we make the assumption that domestic water extraction is negligible ($V_{extract} = 0$) for the relatively scattered rural gathering points extracting comparatively very small water volumes. In addition, irrigation water requirements are minimal during winter months (as it is fallow for farmers) or days when $Precipitation > 0$ (as farmers will not irrigate when rainfall occurs). V_{inflow} calculated by Eqs. (1) and (2), along with all the related observations (e.g. precipitation, water levels), can be used as the accurate value of the total catchment runoff volume to calibrate and validate the corresponding outputs from hydrological modeling. Here, the hydrological period for calibration and validation covers all the possible conditions, including drought, flooding and normal seasons. The optimal parameters are therefore robust, and the simulation is representative for most situations (including drought days in summer).

3.2.2. Calibration and validation

Model calibration and validation are important procedures to improve the reliability of the simulation results. In this paper, we adopt the accepted Sequential Uncertainty Fitting (Sufi2) (Schuol et al., 2008; Song et al., 2016) in SWAT-CUP across nine hydrological parameters (Table S1) to calibrate the simulated daily runoff to the observed daily data at the Duling Station (using 2015 and 2016 data for calibration, and 2014 data for validation). The period from 2014 to 2016 covers all possible hydrological conditions, including a drought season, a flooding period and a normal season. To determine the most suitable hydrological parameters, we ran 1500 cal-

Table 1
Data Sources for the Nandu River SWAT modeling calibration and validation.

Data	Source	Description
Topography	National Geomatics Center of China (http://ngcc.sbsm.gov.cn)	1:1,000,000 DEM of the study region to define major rivers and delineate catchment boundary (see Fig. S2a)
Land Use	National Land Cover Database (http://www.geodata.cn)	Land use at 1:250,000 resolution shown in Fig. S2c
Soil	Data Center for Resources and Environmental Sciences, Chinese Academy of Sciences (RESDC) (http://www.resdc.cn)	Distribution of soil types shown in Fig. S2d
Hydrological Response Units (HRUs)	–	HRUs delineated from topography, land use, and soil classes, see Fig. S2b
Climate	China Meteorological Administration (http://www.cma.gov.cn) and Nandu River Management office (http://swj.gd.gov.cn)	Long term climate data from the Zhanjiang Station. Short term (2014–2016) precipitation data from Duling Station. See Fig. 3 for geographic locations
Flow at Duling Station	Nandu River Management office (http://swj.gd.gov.cn)	Observed flow measurements at the Duling hydro-meteorological station
Flow at Sluice	Nandu River Management Office (http://swj.gd.gov.cn)	Computed through reservoir daily water volume

ibration iterations to maximize the common coefficient of determination (R^2) and the Nash-Sutcliffe (NS) coefficient as objective functions (Abbaspour et al., 2004). For these coefficients, R^2 ranges between 0 and 1, with higher values indicating a closer fit. NS ranges from $-\infty$ to 1, with NS ≥ 0.75 regarded as a 'good' fit, 0.36–0.75 as 'satisfactory', and NS < 0 as 'unacceptable' (Santhi et al., 2010).

An overview of the results of the calibration and validation processes at the Duling Station and sluice outlet is presented in Table 2. The adopted model parameters are given in Table S1 and a detailed breakdown of volumetric measurements is provided in Table S2. The daily time series calibration and validation are presented in Fig. 4.

In both the calibration and validation, R^2 values appear sufficiently accurate with a good linear correlation between the simulated and observed runoffs, albeit with a slightly greater predictive accuracy across the calibration dataset compared to the validation dataset. Similarly, the NS coefficient suggests a good fit to the calibration data and a satisfactory validation for both the Duling station and the sluice outlet. When considering the total volume at the Duling station, the model calibrates within <1% to the observed data and <2% for the validation dataset. With no gauging stations or control structures at the small basin outlet (see Fig. 3) available

for detailed calibration of this small portion of the catchment, the calibrated and validated SWAT model parameters from the larger area are adopted. Overall, we may assume that the resulting parameter sets (Table S1) are reasonable and reliable for this analysis.

3.3. Carbon measurement and stable isotope analysis

3.3.1. Field sampling

To evaluate the C concentration in the Nandu River basin, we collected water samples from across the river system as well as from the dominant land use vegetation (paddy rice and eucalyptus forest). Considering the spatial heterogeneity of the study area, six representative sampling sites (see Fig. 3) were chosen over the whole catchment to capture the C signal. Duling is a site located within the upper tributary system without a significant external influence from the downstream reservoir control practices. The Upstream, Midstream and Sluice sampling sites were selected as the key control points for the river C values in each river section (e.g. the Upstream site was chosen at the tributary junction with relatively stable, continuous river flow). The Fishpond site was chosen to represent the C signal from the fishpond. The small basin Outlet2 site was chosen to capture the C signal from the small

Table 2
Model calibration and validation statistics for discharge (R^2 and NS statistics) and the total volume over the time series (Percent Relative Error, RE).

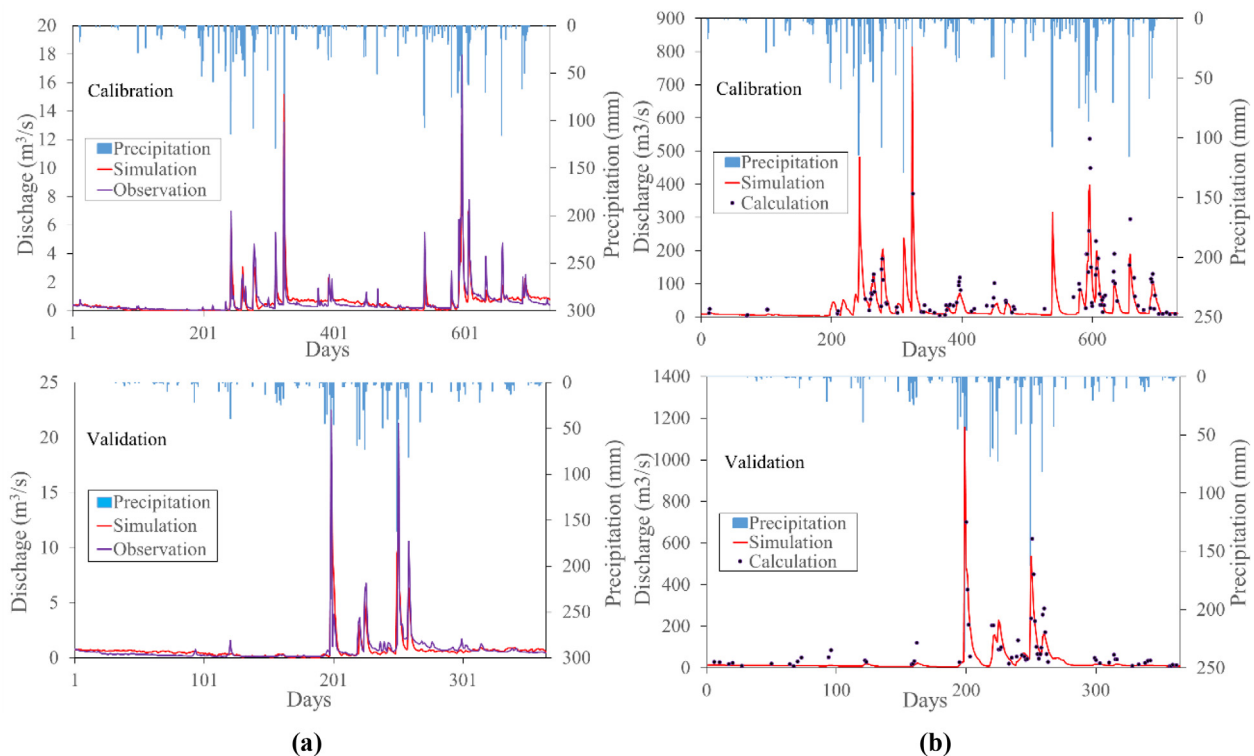| Dataset	Location	Flow Prediction R^2	Flow Prediction NS	Total Volume RE (%)
Calibration (2015/2016)	Duling	0.77	0.77	0.01% (2015) 0.86% (2016)
	Sluice	0.78	0.77	–
Validation (2014)	Duling	0.72	0.71	1.68% (2014)
	Sluice	0.70	0.68	–

Fig. 4. Daily results of the calibration (Jan. 01, 2015 to Dec. 31, 2016) and validation (Jan. 01, 2014 to Dec. 31, 2014) at the (a) Duling hydro-meteorological station (Simulation: model outputs; Observation: observed discharge at the Duling station), and (b) the sluice outlet (Simulation: model outputs; Calculation: inflow to the reservoir V_{inflow}, derived using Eqs. (1) and (2)).

region and the fishpond. In addition, the rice and eucalyptus samples were taken from typical representative land, respectively. To summarize, the spatial distribution of the sampling sites was designed to capture the conditions across the whole catchment.

From the perspective of time scale, samples were taken on three separate occasions to capture the river system undergoing both drought and normal conditions: August 2015 (drought conditions: following a drought with a 139-year return period, Fig. S3 and Section 4.2.2), December 2015 (normal conditions) and September 2016 (normal conditions). Those three field sampling campaigns captured the significant turning points of the yearly C variation. For example, the sampling in Aug. 2015 was carried out at the end of a drought season to obtain the accumulated high C signal due to the extreme drought. The field sampling in Dec. 2015 was conducted in winter time with normal weather conditions to represent the low C concentration signal. The field sampling in Sep. 2016 is representative of the flooding period during which the sluice was almost continuously kept open to release the excess water discharge. At each site, two continuous days of sampling (with three repetitive samples each day) were conducted to ensure the reliability and accuracy of the data.

Samples were subjected to a complex treatment (including for example filtration, inactivation and sealing) and maintained at appropriate temperatures prior to laboratory testing. The water samples were analyzed for concentrations of dissolved organic carbon (DOC), dissolved inorganic carbon (DIC) and particulate organic carbon (POC). The sample bottles, filter paper and glass fibers were burned in a muffle furnace for more than six hours before use to remove organic carbon impurities. The concentration of DIC was measured by TOC-L CPH, with a standard deviation of less than 2%. The concentration of DOC was measured by a TOC analyzer (GE Analytical Instruments) and the measuring error was ±3%. The concentration of POC was measured using the Germany Element Analyze System (GmbH) with a measuring error of ±0.5%. The total C content was acquired by summing the three components.

3.3.2. Stable isotopic analyses

To understand the sources of the riverine C, we further analyzed the ^{13}C isotope content in both the water and crop samples. The δ^{13}C-DIC was measured using a GasBench system coupled with a Finnigan MAT 253 Isotope Ratio Mass Spectrometer (IRMS, Thermo-Fisher Scientific Co., Shanghai, China). The δ^{13}C-DOC was measured using an LC-isolink system coupled with a Finnigan Delta V IRMS (Thermo-Fisher Scientific Co.). The δ^{13}C-POC was measured using a HT/EA 2000 Elemental Analyzer coupled with the Finnigan MAT 253 IRMS, by filtering 1 L of river water into a pre-combusted fiberglass filter.

To analyze the different sources of C in the water samples, we applied the stable isotope mixing model MixSIR (sampling important resampling), which is based on Bayesian analysis taking fractionation factors and uncertainty into consideration (Moore and Semmens, 2008; Jackson et al., 2009). The basic equation of this mixing model (Jackson et al., 2009) is:

$$\delta_M = \sum_{i=1}^{n} f_i(\delta_i + \gamma_i) \quad where \quad \sum_{i=1}^{n} f_i = 1 \tag{3}$$

where δ_M and δ_i represent the stable isotope values of the mixing fluid and the source respectively, f_i is the ratio of each source, γ_i is the fractionation value of this source, and n is the number of sources being mixed. In this study $n = 3$, as we focus on quantifying the C originating from the dominant land uses: paddy rice, eucalyptus and fish ponds. The resulting source δ values are shown in Table S3.

3.4. Combining hydrological modeling and C concentrations/C flux

By combining the runoff data with the C concentrations, it is possible to evaluate the C fluxes in the river. To investigate the impacts of the river system modification on the land-sea C flux during certain periods we consider the mass balance:

$$M_{impact} = M_{inflow} - M_{outflow} - \Delta M_{reservoir} \tag{4}$$

where M_{impact} is the reduction in land-sea C mass transfer arising from water management interventions over a given time period, M_{inflow} is the total mass of incoming C in this period, and $M_{outflow}$ is the land-sea C flux discharged through the sluice gate. $\Delta M_{reservoir}$ is the C mass change of the reservoir, which can be evaluated with the change of the water volumes and C concentrations between the starting and ending time in the given period. Both M_{inflow} and $M_{outflow}$ can be obtained via:

$$M = \sum_{i=1}^{n} (c_i \times V_i) \tag{5}$$

where M represents the total C mass (either M_{inflow} or $M_{outflow}$), c_i is the C concentration (i.e. DOC, DIC or POC), V_i is the daily water volume and n is the number of calculation days. For M_{inflow}, the water volumes are obtained from the catchment hydrological model (V_{inflow}). Similarly, for $M_{outflow}$, the water volumes are determined through the sluice management data ($V_{outflow}$) using Eq. (1).

For dry and wet periods (i.e. the sample data) we can use the laboratory-measured C concentrations for the relatively stable C concentration values. Between these periods, when wet periods change to dry periods, we assume that the C concentration variation is a linear process due to the lack of observational data.

4. Results and analysis

4.1. Carbon concentration analysis

Fig. 5 presents the results of the water sampling performed across the different time periods: (a) Dec. 2015 (normal conditions), (b) Sep. 2016 (normal condition, actually flooding period), and (c) Aug. 2015 (severe drought conditions). These results are shown for the C concentration along the river from Duling to the sluice outlet (left panels) as well as at the three selected sampling sites (right panel).

With respect to the concentration change along the river (Fig. 5, left panels), relatively consistent low-level DOC and POC were observed at the Duling station ($\sim$0.5–2.5 mg C L^{-1}) regardless of the conditions (normal or drought). The DIC is mainly influenced by the atmospheric and water flow conditions and therefore shows significant variation. Given that the Duling station is located within an upper tributary with no influence from the downstream reservoir/sluice control, we suggest that the Duling station can be used to represent an area of the catchment without significant external influences on the land-river C transfer. As the DOC and POC concentrations were observed to remain at a stable low-level in our sampling results, we infer that variations of the quantity of riverine C arising from the primary forest and croplands are determined by the volumes of runoff rather than C concentrations.

In the sluice reservoir, the C concentrations vary significantly between drought and normal seasons. During the normal seasons (Fig. 5a and b), the total observed C concentration was between 4 and 8 mg C L^{-1} in the river from the Duling station to the sluice reservoir. As there were no significant differences in the order of magnitude between Dec. 2015 and Sep. 2016, we collectively classify these values as typical of normal conditions. However, during drought periods the total C showed a cumulative effect and
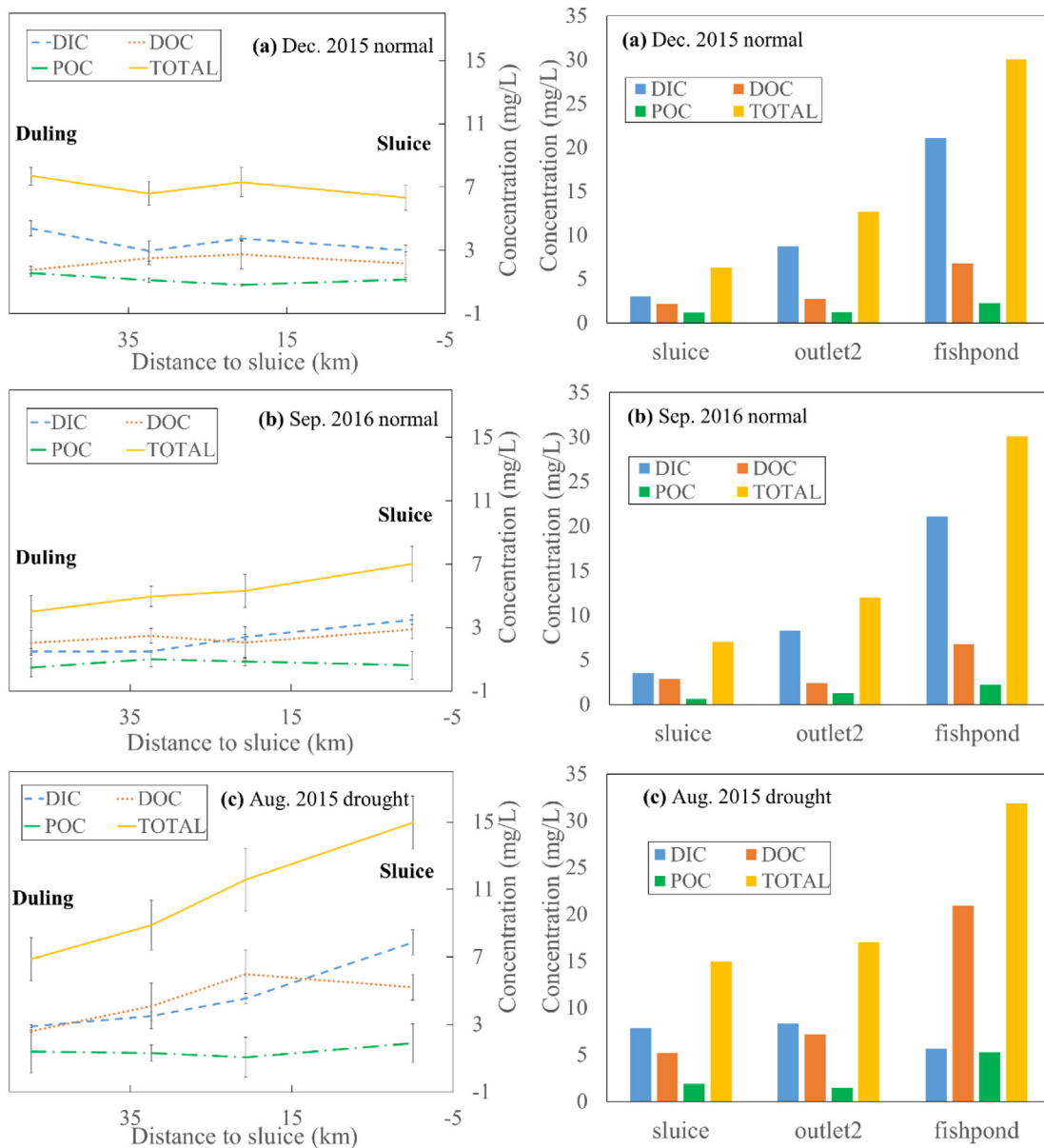
Fig. 5. Changes in C concentration along the river and at different outlets for (a) Dec. 2015 (normal conditions), (b) Sep. 2016 (normal conditions), and (c) Aug. 2015 (severe drought conditions). The four sampling points down the main river channel (left panel figures) represent the Duling, Upstream, Midstream and Sluice sites, as shown in Fig. 3, respectively.

increased significantly downstream, reaching a peak concentration of around 15 mg C L^{-1} at the sluice reservoir.

When we compare the concentrations observed at the two basin outlets (Outlet1 and Outlet2) and the fish pond (Fig. 5, right panels), we measured consistently higher total C concentrations (~30 mg C L^{-1}) in the water discharged from the fish ponds. However, the individual components contributing to the total C concentration vary between these sampling sites. The reasons for this are likely related to corresponding management in fishpond under different climate condition, which is beyond the scope of this paper. This in turn led to comparatively high concentrations at Outlet2 compared to those observed at the sluice gate.

4.2. Impacts of human water management on riverine C flux

Fig. 6 presents the time-series results of our integrated model of the Nandu Basin (detailed in Section 3) for comparing the Total C,

DIC, DOC and POC over 2015 (Fig. 6a) and 2016 (Fig. 6b). These concentrations are modeled at the sluice outlet for current C conditions with human impacts (shown as orange bars) and simulated C conditions without human interventions (shown as black lines). Table 3 provides the summated LSRCT fluxes over the two years shown in Fig. 6.

4.2.1. Human impact under general conditions

Table 3 shows the significantly lower C flux transfer (for all of DIC/DOC/POC/TOC) under current conditions compared to those expected if no human interventions were in place in the catchment. This is apparent for both the full years (Jan.–Dec.) and a reduced time period (Feb.–Jul.), with the range in C concentration from less than 1% to more than 60%. Furthermore, Fig. 6 indicates that without human interventions the natural LSRCT is a smooth and continuous process varying with the water flow, but the current conditions show a more concentrated pattern and a more dis-
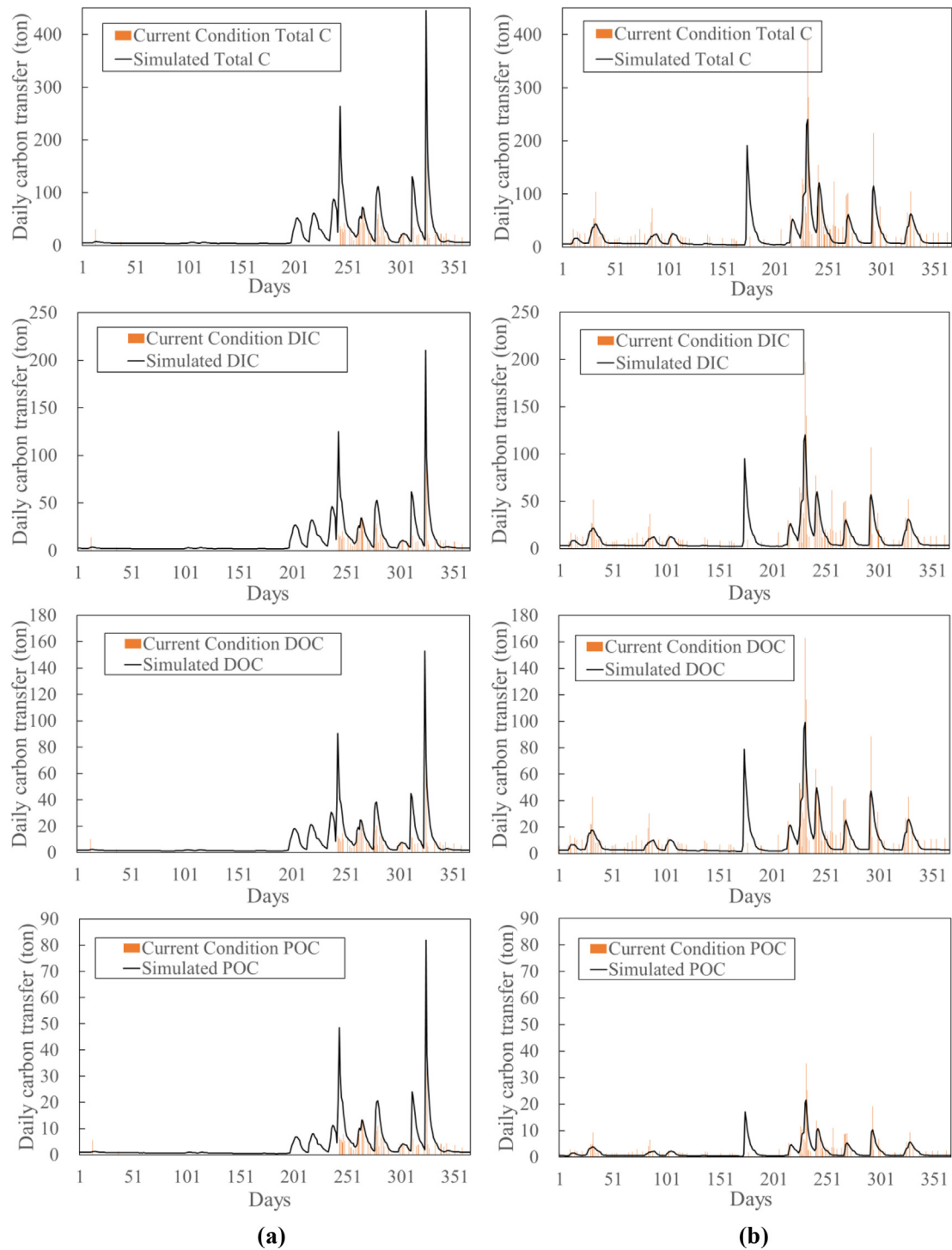
Fig. 6. The daily changes in the DIC, DOC, POC and total C (in ton C/day) during (a) 2015 and (b) 2016. (The black lines represent the simulated C discharges without the influence of the dam and human water use. The orange bars represent the C discharges at the sluice gate from the sluice management data.) (For interpretation of the references to colour in this figure legend, the reader is referred to the web version of this article.)

continuous process, which may affect the ecological environment in the estuarine zone (Lenton, 2000; Doxaran et al., 2009; Chen and Swaney, 2012).

4.2.2. Human impact under drought conditions

As highlighted in Section 4.1, the LSRCT is significantly impacted by human interventions during drought events. By fitting a Pearson Type-III (P-III) statistical distribution (Bai and Fu, 2001; Singh et al., 2005) to the complete dataset (Fig. S3), we estimate return periods of ~1.8 years for the 2015 annual precipitation

(1656.5 mm) and ~1.4 years for the 2016 annual precipitation (1821 mm). Although these appear superficially to be regular years, an interesting observation arises when we examine the dataset on only drought monthly timescale. For example, we observe a 139-year return period drought in 2015 during the time-frame Feb. 01 – Jul. 31 and a 5-year return period drought in 2016 (Fig. S3).

On an annual timescale, Table 3 shows that under conditions of no human intervention, the natural LSRCT was expected to be 7430 ± 1140 tons in 2015 (with 1657 mm precipitation and a

Table 3
LSRCT (tons) at the sluice station under current conditions and without the human interventions.

Data	Year	Scenario	DIC	DOC	POC	TOC	Impact Percentage
Jan. 1 to Dec. 31	2015	Without Interventions	3608 ± 554	2556 ± 392	1266 ± 194	7430 ± 1140	–
		Current Conditions	823 ± 107	583 ± 76	289 ± 38	1695 ± 221	23 ± 5%
	2016	Without Interventions	3823 ± 587	3160 ± 485	685 ± 105	7667 ± 1176	–
		Current Conditions	2346 ± 306	1939 ± 253	420 ± 55	4705 ± 614	61 ± 11%
Feb. 1 to Jul. 31	2015	Without Interventions	575 ± 88	394 ± 60	170 ± 26	1140 ± 175	–
		Current Conditions	3.6 ± 0.5	2.6 ± 0.3	1.4 ± 0.2	7.7 ± 1.0	0.7 ± 0.1%
	2016	Without Interventions	1190 ± 183	984 ± 151	213 ± 33	2387 ± 366	–
		Current Conditions	444 ± 58	367 ± 48	80 ± 10	890 ± 116	37 ± 7%

1.76-year drought) and 7667 ± 1176 tons in 2016 (with 1821 mm precipitation and a 1.41-year drought) and there was no significant difference in terms of the rainfall amount. However, the results change distinctly when we examine current conditions with human interventions in place in the catchment. We observed only 1695 ± 221 tons C (23 ± 5% of the estimate for no-intervention conditions) in drought year 2015 compared to 4705 ± 614 tons C (61 ± 11% of the estimate for no-intervention conditions) in normal year 2016.

On seasonal timescales, the human impacts on the LSRCT are more significant during drought periods. For example, during the drought that occurred during the period 01/02–31/07 in 2015 (a 139-year drought), only 0.7 ± 0.1% (7.7 ± 1.0 tons) of the riverine

C was discharged to the sea via the sluice outlet. The additional riverine carbon that was not transported to the sea (1132 ± 175 tons) was reduced during this 139-year return period drought event. The period Feb. 01–Jul. 31 of 2016 constituted only a 5-year return period drought, nevertheless a significant proportion of the riverine C (37 ± 7%) was not discharged to the ocean (Table 3).

4.3. Stable isotopic results and analysis

We have noted that modifications to land use and human interventions on the hydrology of the Nandu River basin have had a major impact on the LSRCT. We further investigated the sources
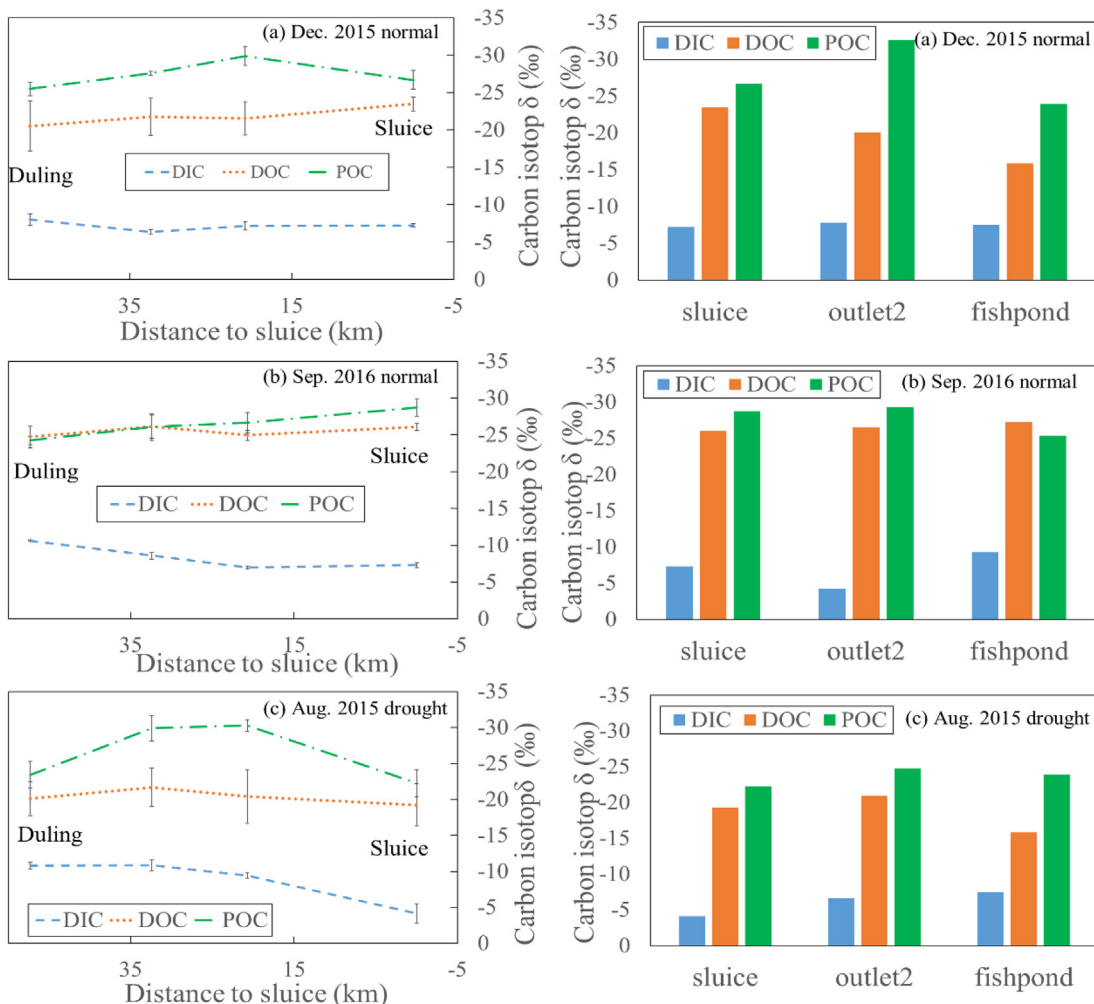

Fig. 7. Stable C isotope ratio of the three carbon forms along the river and at different sites according to the samples taken in (a) Aug. 2015, (b) Dec. 2015, and (c) Sep. 2016 (the four sampling sites in the main river channel from left to right correspond to Duling, Upstream, Midstream and Sluice, respectively).
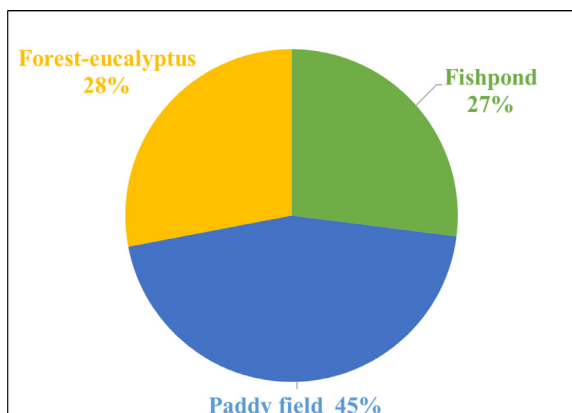
Fig. 8. POC source composition in 2016 at the sluice.

of C and the contribution of different land uses during both drought and non-drought conditions using stable isotopic analysis. The isotope δ values of the water samples along the river and at the same selected sampling sites as Fig. 3 are shown in Fig. 7.

During drought conditions, the δ^{13}C-DIC values ranged from -12.42 to $-2.43‰$ (Fig. 7c). The isotopic value gradually increased towards the sluice, presumably due to the dissolution of CO_2 along the river in which C fractionation could take place, with the δ^{13}C-DIC reaching as high as $-1.1‰$ (Deuser and Degens, 1967; Halas et al., 1997). Using the DIC concentration (7.87 mg C L^{-1}), the pH (7.79–8.08) and the water temperature (31 °C), the partial pressure of CO_2 (pCO_2) was calculated (CO2SYS-Program (Lewis and Wallace, 1998)) as 174.3 µatm, which is much lower than the atmospheric CO_2 pressure of 393 µatm. During the extreme drought, the sluice was closed for several months, providing enough time for the dissolution of CO_2 within the reservoir. The observed DIC isotope value of the sluice was therefore most likely a mixture of the upstream signal and the atmospheric interaction, which are hard to distinguish. During normal conditions (Fig. 7a and b), the sluice was frequently opened and retention time for solution was limited, which could also be a possible explanation for the similar C concentration during the two periods of normal conditions.

The observed variation in δ^{13}C-DOC was small between the upstream and downstream sampling sites ($-19‰$ to $-26‰$), irrespective of the season. The DOC in the river largely originates from soil organics or other sources (-21 to $-16‰$) (Osburn and Gilles, 2007) and could be altered by the degradation fractionation of microorganisms and plankton in the water (Blair et al., 1985; Erez et al., 1998). Nevertheless, the soil organic C can be changed by fertilization in cropland, and microorganisms and plankton can be influenced by the flow velocity, which can be controlled by the sluice.

Across the Nandu River Basin, the sources of POC include rice paddies, eucalyptus forest trees and fishponds with little δ-value fractionation along the river. The rice paddies and the fishponds are each mainly controlled by human management. A traceability analysis of POC was carried out using the MixSIR model. Results showed that C from the rice paddies (45 ± 5%) and fishponds (27 ± 5%) combined accounted for 72 ± 5% of the POC (Fig. 8). This demonstrates that human-controlled land-use types such as these have a significant influence on the LSRCT in such a small coastal basin. In reality, during major droughts in the area, fishponds are usually unused given the significant requirement for fresh water. At such times, the POC originating from the fishponds is limited, with rice paddies contributing around 62 ± 5% of the total POC, albeit at a reduced total amount of C due to the decreased land C sources.

5. Conclusions

By performing coupled hydrological modeling, field sampling, and stable isotope analysis, this study assessed the impacts of human water management strategies on the LSRCT in coastal basins. The case study of the Nandu River basin illustrates that this coupled framework is an effective approach to assess the LSRCT. We find that human water management has significant impacts on LSRCT and plays a dominant role in our study area. At both annual and seasonal timescales, the LSRCT is reduced by a significant proportion due to human water management, while drought conditions evidently enhance these human impacts. We draw the following conclusions from this research:

(1) (1) The foundation of the framework lies in the calibrated and validated hydrological processes. Within this framework, determining how to simulate the human water management practices is of great importance. In coastal areas, water resources and runoff are highly controlled by human water management strategies rather than natural processes. Hydrological modeling is an effective tool to restore the natural runoff processes and eliminate the effects of human impacts. The Nandu River basin application had the advantage of the availability of an empirical equation to describe the capacity of the sluice reservoir and make assumptions regarding conditions without human interventions (i.e. no irrigation during winter or when P > 0), when calibrating and validating the model.

(2) (2) The incoming C concentrations from different sources (e.g. forest, agriculture) have little seasonal changes therefore the variations of C are dominated by the controlled volumes of runoff (e.g. resulting from dam construction or irrigation) rather than C concentrations, consistent with existing literature (Raymond and Oh, 2007; Raymond et al., 2008). In contrast, under drought conditions, a significant increase in total C concentrations (up to 2 times higher) may be observed. This increased concentration is likely caused by two factors: (i) the increased evaporation of water at the sluice reservoir with little water reaching the ocean (e.g. from Jan. to Aug. 2015, the sluice gate was kept closed, except for a 4-hour opening on Jan. 13 and a 1-hour opening on Feb. 06 in our case study); (ii) the slower river flow velocity throughout the catchment, leading to increased aeration at the reservoir and the gradual dissolution of CO_2.

(3) (3) The C sources under human water management control (e.g. agriculture and aquaculture) can contribute a dominant proportion of POC, whether in drought (for example 62 ± 5% of POC in our case study) or normal (72 ± 5% of POC in our case study) conditions. In order to determine the sources of DOC and DIC in future research, an accurate model for the isotope fractionation and diversion during the transfer process should be developed, to better understand the mechanisms behind these anthropogenic activities.

(4) (4) The total LSRCT is significantly impacted by human water management, whether at the seasonal scale (for example a 99.3 ± 0.1% reduction accompanying a 139-year drought in our case study) or at the annual scale (a 39 ± 11% reduction in the normal year and a 77 ± 5% reduction in the drought year in our case study), and drought can significantly enhance this human impact. In detail, the total water demand for irrigation or fishponds during drought conditions is higher than in normal conditions, such that stricter water management strategies are required to reserve fresh-

water and the C transfer is impacted in this way. In addition, the C concentration is higher during drought periods and the human impacts increase along with this.

6. Discussion and perspective

Our case study illustrates that an integrated framework incorporating hydrological modeling, field sampling and isotope analysis can quantitatively assess the river discharge and LSRCT processes under natural conditions (without human intervention) as well as current conditions (with human intervention) in coastal basins. Overall, we note some limitations in our research approach associated with simplifying assumptions and omitted calculations. Firstly, the possibility of incorporating all salient factors (e.g. rainfall, irrigation) in the case study in addition to groundwater interactions and industrial/domestic water uses should be explored in future analyses. While this may lead to difficulties when applying the method to more complicated and larger river basins, the insights gained in this analysis demonstrate the advantages of being able to quantify the impact of human activities on LSRCT. Moreover, increased sampling over a longer period of time would be beneficial in future studies following this proposed framework. Accessibility, along with the significant time and cost commitments for collecting samples and laboratory testing, were major constraints in this project (see Section 3.3.1) and these factors may persist in the case of future applications. Automatic sampling instruments should be adopted in further studies to ensure higher sampling rates with shorter space distances between each sampling site, in order to capture the spatial-temporal variability. This will also contribute to a greater understanding of the variation of C concentrations between normal and drought conditions, which was assumed to be linear in this study. In addition, the integrated framework can be supplemented in order to make precise forecasts for the LSRCT process, which could be aimed to assist with various government policies and environmental goals, with the ultimate aim of proposing optimization management measures for sustainable river–offshore development.

Nevertheless, the results of C transfer calculations obtained through this framework are still subject to uncertainty arising from several sources. The industrial and domestic water consumption were neglected and these could have some impact on the water flow simulations, and thus the C flux results. The manual field sampling may also introduce some uncertainty due to the spatial heterogeneity of C and sediment within the river. This can directly influence the C concentration results, resulting in uncertainty in the total C transfer assessment. Multiple repeated sampling campaigns and standard measurements could minimize this uncertainty. Moreover, the model itself contains empirical formulas and complicated parameters to enable simplification. These simplifications, as well as the weakness of the SWAT model in drought simulations, could introduce some uncertainty in the water flow simulation results and eventually influence the C transfer flux calculations. However, performing independent calibration for drought processes to improve the hydrological simulation process may dramatically decrease the uncertainty of the model simulations. The Duling station data used for the model calibration and validation for the whole basin may also introduce some uncertainty. When extended to other basins, this uncertainty could be reduced by using more observation station data for the calibration step. In the stable isotope analysis, we did not consider the isotope fractionation due to its small magnitude, and this may impact on the POC isotope results.

In spite of this, the general framework and methodology presented here are applicable and suitable for other, larger basins, with more complicated natural–built environment interactions. We suggest that future applications should incorporate agricul-tural, aquacultural, forestry and even isotope models into the presented framework for other larger-scale basins, along with further exploration and simulation of various constructive measures to reduce the negative impacts of human interventions on terrestrial and coastal environments. These steps will make important additional contributions to the research field and to our understanding of LSRCT.

Declaration of Competing Interest

The authors declare that they have no known competing financial interests or personal relationships that could have appeared to influence the work reported in this paper.

Appendix A. Supplementary data

Supplementary data to this article can be found online at https://doi.org/10.1016/j.scitotenv.2019.134735.

References

Abbaspour, K.C., Johnson, C.A., Van Genuchten, M.T., 2004. Estimating uncertain flow and transport parameters using a sequential uncertainty fitting procedure. Vadose Zone J. 3, 1340–1352.

Aitkenhead, J.A., Mcdowell, W.H., 2000. Soil C: N ratio as a predictor of annual riverine DOC flux at local and global scales. Global Biogeochem. Cycles 14, 127–138.

Alin, S.R., Rasera, M.D.F.F., Salimon, C.I., Richey, J.E., Holtgrieve, G.W., Krusche, A.V., et al., 2011. Physical controls on carbon dioxide transfer velocity and flux in low-gradient river systems and implications for regional carbon budgets. J. Geophys. Res. Biogeosci., 116

Bai, S.G., Fu, H., 2001. Adaptability study of type P-III curve pattern parameters. Hydroelectric Energy 19, 52–54.

Blair, N., Leu, A., Muñoz, E., Olsen, J., Kwong, E., Des, M.D., 1985. Carbon isotopic fractionation in heterotrophic microbial metabolism. Appl. Environ. Microbiol. 50, 996–1001.

Bouwman, A.F., Bierkens, M.F.P., Griffioen, J., Hefting, M.M., 2013. Nutrient dynamics, transfer and retention along the aquatic continuum from land to ocean: towards integration of ecological and biogeochemical models. Biogeosciences 10, 1–22.

Cai, Y., Guo, L., Wang, X., Aiken, G., 2015. Abundance, stable isotopic composition, and export fluxes of DOC, POC, and DIC from the Lower Mississippi River during 2006–2008. J. Geophys. Res. Biogeosci. 120, 2273–2288.

Canadell, J.G., Le Quéré, C., Raupach, M.R., Field, C.B., Buitenhuis, E.T., Ciais, P., et al., 2007. Contributions to accelerating atmospheric CO2 growth from economic activity, carbon intensity, and efficiency of natural sinks. Proc. Natl. Acad. Sci. 104, 18866–18870.

Chahor, Y., Casalí, J., Giménez, R., Bingner, R.L., Campo, M.A., Goñi, M., 2014. Evaluation of the AnnAGNPS model for predicting runoff and sediment yield in a small Mediterranean agricultural watershed in Navarre (Spain). Agric. Water Manag. 134, 24–37.

Chen, C.A., Swaney, D.P., 2012. Terrestrial-ocean transfers of carbon and nutrient across the coastal boundary. Curr. Opin. Environ. Sustainability 4, 159–161.

Csank, A.Z., Czimczik, C.I., Xu, X., Welker, J.M., 2019. Seasonal patterns of riverine carbon sources and export in NW Greenland. J. Geophys. Res. Biogeosci. 124, 840–856.

Darnaude, A.M., 2005. Fish ecology and terrestrial carbon use in coastal areas: implications for marine fish production. J. Anim. Ecol. 74, 864–876.

Deuser, W.G., Degens, E.T., 1967. Carbon Isotope Fractionation in the System CO2 (gas)-CO2(aqueous)-HCO3-(aqueous). Nature 215, 1033–1035.

Dittmar, T., Kattner, G., 2003. The biogeochemistry of the river and shelf ecosystem of the Arctic Ocean: a review. Mar. Chem. 83, 103–120.

Doxaran, D., Froidefond, J.M., Castaing, P., Babin, M., 2009. Dynamics of the turbidity maximum zone in a macrotidal estuary (the Gironde, France): observations from field and MODIS satellite data. Estuar. Coast. Shelf Sci. 81, 321–332.

Dutta, S., Sen, D., 2018. Application of SWAT model for predicting soil erosion and sediment yield. Sustainable Water Resour. Manage. 4, 1–22.

Erez, J., Bouevitch, A., Kaplan, A., 1998. Carbon isotope fractionation by photosynthetic aquatic microorganisms: experiments with Synechococcus PCC7942, and a simple carbon flux model. Can. J. Bot. 76, 1109–1118.

Gikas, G.D., Yiannakopoulou, T., Tsihrintzis, V.A., 2006. Modeling of non-point source pollution in a Mediterranean drainage basin. Environ. Model. Assess. 11, 219–233.

Goldsmith, S.T., Lyons, W.B., Harmon, R.S., Harmon, B.A., Carey, A.E., McElwee, G.T., 2015. Organic carbon concentrations and transport in small mountain rivers, Panama. Appl. Geochem. 63, 540–549.

Green, R.E., Bianchi, T.S., Dagg, M.J., Walker, N.D., Breed, G.A., 2006. An organic carbon budget for the Mississippi River turbidity plume and plume contributions to air-sea CO_2 fluxes and bottom water hypoxia. Estuaries Coasts 29, 579–597.

Halas, S., Szaran, J., Niezgoda, H., 1997. Experimental determination of carbon isotope equilibrium fractionation between dissolved carbonate and carbon dioxide. Geochim. Cosmochim. Acta 61, 2691–2695.

Hruska, J., Krám, P., McDowell, W.H., Oulehle, F., 2009. Increased dissolved organic carbon (DOC) in Central European streams is driven by reductions in ionic strength rather than climate change or decreasing acidity. Environ. Sci. Technol. 43, 4320–4326.

Jackson, A.L., Inger, R., Bearhop, S., Parnell, A., 2009. Erroneous behaviour of MixSIR, a recently published Bayesian isotope mixing model: a discussion of Moore & Semmens (2008). Ecol. Lett. 12, E1–E5.

Lanen, H.A.J.V., Laaha, G., Kingston, D.G., Gauster, T., Loon, A.F.V., 2016. Hydrology needed to manage droughts: the 2015 European case. Hydrol. Process. 30, 3097–3104.

Lenton, T.M., 2000. Land and ocean carbon cycle feedback effects on global warming in a simple Earth system model. Tellus B: Chem. Phys. Meteorol. 52, 1159–1188.

Lewis, E., Wallace, D. CO2SYS-Program developed for the CO2 system calculations. Carbon Dioxide Inf Anal Center Report ORNL/CDIAC-105, 1998.

Li, M., Peng, C., Wang, M., Xue, W., Zhang, K., Wang, K., et al., 2017. The carbon flux of global rivers: a re-evaluation of amount and spatial patterns. Ecol. Ind. 80, 40–51.

Lin, B., Chen, X., Yao, H., Chen, Y., Liu, M., Gao, L., et al., 2015. Analyses of landuse change impacts on catchment runoff using different time indicators based on SWAT model. Ecol. Ind. 58, 55–63.

Loucks, D.P., Van Beek, E., 2017. Water Resource Systems Planning and Management: An Introduction to Methods, Models, and Applications. Springer.

Mahlknecht, J., Merchán, D., Rosner, M., Meixner, A., Ledesma-Ruiz, R., 2017. Assessing seawater intrusion in an arid coastal aquifer under high anthropogenic influence using major constituents, Sr and B isotopes in groundwater. Sci. Total Environ. 587, 282–295.

Marques, J.S., Dittmar, T., Niggemann, J., Almeida, M.G., Gomez-Saez, G.V., Rezende, C.E., 2017. Dissolved black carbon in the headwaters-to-ocean continuum of Paraíba do Sul River, Brazil. Front. Earth Sci. 5, 11.

Mcgillis, W.R., Hsueh, D.Y., Zheng, Y., Markowitz, M., Gibson, R., Bolduc, G., et al., 2015. Carbon transport in rivers of southwest Haiti. Appl. Geochem. 63, 563–572.

Meybeck, M., 1982. Carbon, nitrogen, and phosphorus transport by world rivers. Am. J. Sci. 282, 401–450.

Mondro, C., 2010. Transport of Organic Carbon from the Tropical Volcanic Island of Dominica. The Ohio State University, Lesser Antilles.

Moore, J.W., Semmens, B.X., 2008. Incorporating uncertainty and prior information into stable isotope mixing models. Ecol. Lett. 11, 470–480.

Ni, H.G., Lu, F.H., Luo, X.L., Tian, H.Y., Zeng, E.Y., 2008. Riverine inputs of total organic carbon and suspended particulate matter from the Pearl River Delta to the coastal ocean off South China. Mar. Pollut. Bull. 56, 1150–1157.

Noacco, V., Wagener, T., Worrall, F., Burt, T.P., Howden, N.J.K., 2017. Human impact on long-term organic carbon export to rivers. J. Geophys. Res. Biogeosci. 122, 947–965.

Osburn, C.L., Gilles, S.J., 2007. The use of wet chemical oxidation with high-amplification isotope ratio mass spectrometry (WCO-IRMS) to measure stable isotope values of dissolved organic carbon in seawater. Limnol. Oceanogr. Methods 5, 296–304.

Pan, Y., Birdsey, R.A., Fang, J., Houghton, R., Kauppi, P.E., Kurz, W.A., et al., 2011. A large and persistent carbon sink in the world's forests. Science 333, 988–993.

Peng, J., Xu, F., Yuan, S., Chen, X., 2002. Discussion on Solving the Drought Problem in the Southwest of Leizhou Peninsula. Water Resour. Prot. 1, 33–36.

Pingram, M.A., Collier, K.J., Hamilton, D.P., David, B.O., Hicks, B.J., 2012. Carbon sources supporting large river food webs: a review of ecological theories and evidence from stable isotopes. Freshwater Rev. 5, 85–104.

Qin, Z.J., Chen, R., 2011. Comprehensive optimization of general arrangement plan of Nandu River's sluice. Sci-Tech Inf. Develop. Econ. 21, 204–206.

Quéré, C.L., Raupach, M.R., Canadell, J.G., Marland, G., Bopp, L., Ciais, P., et al., 2009. Trends in the sources and sinks of carbon dioxide. Nat. Geosci. 2, 831–836.

Ran, L., Lu, X.X., Sun, H., Han, J., Li, R., Zhang, J., 2013. Spatial and seasonal variability of organic carbon transport in the Yellow River, China. J. Hydrol. 498, 76–88.

Raymond, P.A., Oh, N., Turner, R.E., Broussard, W., 2008. Anthropogenically enhanced fluxes of water and carbon from the Mississippi River. Nature 451, 449–452.

Raymond, P.A., Oh, N.H., 2007. An empirical study of climatic controls on riverine C export from three major US watersheds. Global Biogeochem. Cycles 21.

Regnier, P., Friedlingstein, P., Ciais, P., Mackenzie, F.T., Gruber, N., Janssens, I.A., et al., 2013. Anthropogenic perturbation of the carbon fluxes from land to ocean. Nat. Geosci. 6, 597–607.

Richey, J.E., Hedges, J.I., Devol, A.H., Quay, P.D., Victoria, R., Martinelli, L., et al., 1990. Biogeochemistry of carbon in the Amazon River. Limnol. Oceanogr. 35, 352–371.

Santhi, C., Arnold, J.G., Williams, J.R., Dugas, W.A., Srinivasan, R., Hauck, L.M., 2010. Validation of the swat model on a large RWER basin with point and nonpoint sources. Jawra J. Am. Water Resour. Assoc. 37, 1169–1188.

Schuol, J., Abbaspour, K.C., Yang, H., Srinivasan, R., Zehnder, A.J.B., 2008. Modeling blue and green water availability in Africa. Water Resour. Res. 44, 212–221.

Semiletov, I.P., Pipko, I.I., Shakhova, N.E., Dudarev, O.V., Pugach, S.P., Charkin, A.N., et al., 2011. Carbon transport by the Lena River from its headwaters to the Arctic Ocean, with emphasis on fluvial input of terrestrial particulate organic carbon vs. carbon transport by coastal erosion. Biogeosciences 8, 2407–2426.

Setegn, S.G., Srinivasan, R., Melesse, A.M., Dargahi, B., 2010. SWAT model application and prediction uncertainty analysis in the Lake Tana Basin, Ethiopia. Hydrol. Processes 24, 357–367.

Singh, V.P., Wang, S.X., Zhang, L., 2005. Frequency analysis of nonidentically distributed hydrologic flood data. J. Hydrol. 307, 175–195.

Song, Z., Zeng, J., Jin, Y., Hu, X., Sun, D., Lu, S., et al., 2016. Distributed simulation of monthly runoff using SWAT and SUFI-2 algorithm in Shiyang River Basin. Bull. Soil Water Conserv. 36, 172–177.

Srinivasan, R., Ramanarayanan, T.S., Arnold, J.G., Bednarz, S.T., 1998. Large area hydrologic modeling and assessment part II: model application. Jawra J. Am. Water Resour. Assoc. 34, 91–101.

Tian, H., Yang, Q., Najjar, R.G., Ren, W., Friedrichs, M.A., Hopkinson, C.S., et al., 2015. Anthropogenic and climatic influences on carbon fluxes from eastern North America to the Atlantic Ocean: a process-based modeling study. J. Geophys. Res. Biogeosci. 120, 757–772.

Tibebe, D., Bewket, W., 2011. Surface runoff and soil erosion estimation using the SWAT model in the Keleta watershed, Ethiopia. Land Degrad. Dev. 22, 551–564.

Volpi, E., Fiori, A., Grimaldi, S., Lombardo, F., Koutsoyiannis, D., 2016. One hundred years of return period: strengths and limitations. Water Resour. Res. 51, 8570–8585.

Walling, D.E., 2006. Human impact on land-ocean sediment transfer by the world's rivers. Geomorphology 79, 192–216.

Wassenaar, L.I., Athanasopoulos, P., Hendry, M.J., 2011. Isotope hydrology of precipitation, surface and ground waters in the Okanagan Valley, British Columbia, Canada. J. Hydrol. 411, 37–48.

Wu, Y., Zhang, J., Liu, S.M., Zhang, Z.F., Yao, Q.Z., Hong, G.H., et al., 2007. Sources and distribution of carbon within the Yangtze River system. Estuar. Coast. Shelf Sci. 71, 13–25.

Xia, B., Zhang, L., 2011. Carbon distribution and fluxes of 16 rivers discharging into the Bohai Sea in summer. Acta Oceanol. Sin. 30, 43.

Zhang, D., Chen, X., Yao, H., Lin, B., 2015. Improved calibration scheme of SWAT by separating wet and dry seasons. Ecol. Model. 301, 54–61.

Zhang, D., Zhang, W., Zhu, L., 2005. Improvement and application of SWAT-A physically based, distributed hydrological model. Sci. Geogr. Sinica 25, 434–440.

Zhang, L.J., Wang, L., Cai, W.J., Liu, D.M., Yu, Z.G., 2013. Impact of human activities on organic carbon transport in the Yellow River. Biogeosciences 10, 2513–2524.